ACS APPLIED ELECTRONIC MATERIALS

pubs.acs.org/acsaelm

Article

Copper Electrodes via 3D Printing and Laser Sintering Fabrication for Nonenzymatic Glucose Detection

Priscila S. L. Silva, Diele A. G. Araujo, Débora N. Medeiros, Rômulo A. Ando, Lauro A. Pradela-Filho,* and Thiago R. L. C. Paixão*

Cite This: https://doi.org/10.1021/acsaelm.5c00862

Read Online

ACCESS | Metrics & More | Article Recommendations | Supporting Information

ABSTRACT: Glucose is considered an important marker for medical and food applications. Usually, glucose quantification is performed using a copper wire electrode. However, considering the growing demand for point-of-need analyses, the fabrication of disposable sensors has become an emerging technology. This study reports on the fabrication of disposable copper electrodes by combining fusion deposition modeling (FDM) 3D printing and laser sintering (LS). A copper/polylactic acid plate was first printed using an FDM 3D printer. Subsequently, a specific surface area was precisely sintered using an infrared (IR) laser engraving machine, resulting in an electrically conductive copper film, as confirmed by voltammetry and scanning electron microscopy characterizations. The laser processing parameters were optimized considering sensor sensitivity for glucose oxidation through amperometric measurements. The best parameters included the 1.6 W laser power, 5 mm s^{-1} scan rate, 12 mm height, and 0.1750 mm distance between the laser engraver's beamlines. Under optimum experimental conditions, the electrodes showed a linear response from 0.5 to 7.5 mmol L^{-1} glucose, with their analytical applicability further demonstrated for the analysis of oral rehydration solution samples. Therefore, this work presents a straightforward approach for fabricating disposable copper electrode surfaces, offering rapidity, versatility, and potential utility for sensing applications beyond glucose quantification.

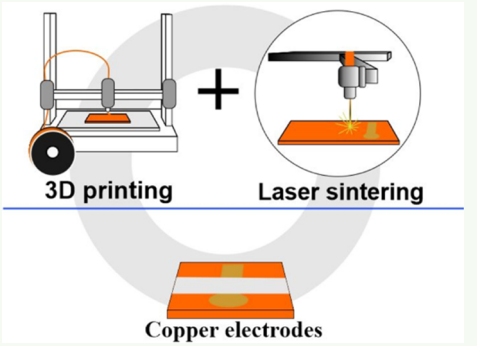

KEYWORDS: *3D-printed electrodes, electrochemical sensors, laser treatment, disposable electrodes, drink samples*

1. INTRODUCTION

High-quality metallic films are conventionally patterned by chemical vapor deposition (CVD) or physical vapor deposition (PDV).[1] CVD involves depositing the film from a chemical reaction with gas precursors.[2] In the PVD process, the precursors are vaporized from a solid or a liquid, followed by metal deposition onto the desired substrate. Sputtering deposition is a PVD technique. These techniques are combined with the lithography processes, resulting in systems with different sizes and formats.[3] Despite producing high-precision conductive films and coatings, the fabrication processes are typically conducted in cleanroom facilities, making electrode production unaffordable in most research laboratories from underdeveloped countries because of the high investment exceeding US$1 million.[3]

Considering its affordability, 3D printing is an emerging technique for the mass production of electrochemical sensors.[4−7] Fused deposition modeling (FDM) is a 3D printing technique widely used to fabricate electrodes. The process initiates with a virtual image of a 3D object projected with computer-aided design (CAD) software, such as Fusion 360, Autodesk Inventor, or Tinkercad. This image is converted to an STL file, which is sliced into sequential 2D layers, producing a G-code file for the 3D printing machine. The printing consists of the layer-by-layer deposition process of the extruded thermoplastic filament. The deposition results in several stacked layers, generating the 3D object.

For electrode fabrication, the filament composition consists of a mixture of a binding polymer and carbon source or metal particles. Acrylonitrile butadiene styrene (ABS) and polylactic acid (PLA) are binders ordinarily present in commercial filaments. Commercial conductive carbon filaments are composed of carbon black or graphene, while metal-filled filaments are based on iron, steel, copper, brass, and bronze. Despite the availability, commercial metal-filled filaments often exhibit low electrical conductivity[8] or lack it entirely,[9,10] requiring thermal processing to enhance their electrical properties after printing. Multi3D company commercializes high-conductivity copper filaments. However, a 100 g spool costs US$ 215.00, limiting the sensor fabrication in research laboratories with resource restrictions.

Received: April 28, 2025
Revised: June 4, 2025
Accepted: June 29, 2025

In this sense, the present work reports the fabrication of disposable copper electrodes through a two-step automated process, starting with FDM 3D printing followed by CO_2 laser sintering. Such an integration is a promising option for precisely replicating the electrode pattern, offering affordability and rapidness.[11] The prices of FDM printers and laser engraving machines were searched on the Amazon Web site to exemplify the resulting combination cost. FDM printers for beginners can be acquired for ∼US$ 180.00 (Creality and Tronxy printers), while a laser engraving machine costs ∼US$ 500.00. Hence, combining both machines can potentially automate electrode fabrication, reducing processing costs and time. Laser sintering has been explored for carbon electrode treatment,[12] metal ink sintering,[13] and electrode surface modification with metallic nanoparticles.[14−16] However, this technology has not yet been applied to sintering copper filament electrodes.

The resulting copper electrodes were explored for glucose oxidation, verifying their accuracy for rehydration sample analyses. Glucose determination is highly relevant for medical and food purposes.[15,17] Glucose electrochemical quantification can be conducted using enzymatic[18,19] or metallic electrodes,[15,20,21] such as gold,[15] platinum,[22] and copper.[21] Among the metallic electrodes, copper offers higher accessibility, while also providing good sensitivity and selectivity to glucose.[21] Redondo et al.[9] fabricated fully metallic copper 3D-printed electrodes for glucose quantification. The electrodes were sintered via thermal treatment. The process required a high-temperature furnace, which burned the insulating binding parts, converting the printed material into a metallic form.[9,10] Despite its effectiveness, this process is time-consuming, and the entire printed material is sintered, which affects scalability and limits the versatility of 3D-printed structures. Kumar et al.[23] patterned copper-plated 3D-printed electrodes for glucose quantification. For this, 3D-printed graphene/PLA electrodes were subjected to modification by the electrodeposition process. Such a process was accomplished by applying a potential sufficiently negative to reduce the copper ions present in the solution, depositing a metallic film at the electrode surface. The deposition was conducted under constant stirring. During deposition, the morphological aspects of the copper film can be modulated by adjusting solution pH, temperature, supporting electrolyte composition, copper concentration, applied potential, and deposition time.[24] The mentioned modification approach has also been applied to glassy carbon[24] and screen-printed electrodes.[25] Despite its simplicity, this fabrication method is laborious, hindering the scalable production of disposable electrodes. While commercial copper electrodes are available and can be used for analysis,[26] disposable sensors are necessary for out-of-lab analysis, highlighting the significance of this work. Therefore, this study presents an alternative method for patterning disposable copper filament electrodes via 3D printing and laser sintering, thereby opening up possibilities for other analytical applications.

2. EXPERIMENTAL SECTION

2.1. Chemicals and Materials. The solutions were prepared with purified water (18.3 MΩ·cm) from Direct-Q 5 Ultrapure Water Systems (Millipore, MA). All chemicals (analytical grade) were used without any additional purification. Glucose, sodium nitrite, sodium sulfite, and saccharose were purchased from Merck (Darmstadt, Germany), and potassium hydroxide from Nuclear. Ascorbic acid and maltose were acquired from Sigma-Aldrich (St Louis, MO, USA). A hot glue gun was acquired in a local market. The acccreate copper-filled filament was bought from Weistek.

2.2. Printing and Laser Sintering of Copper Electrodes. The fabrication process of copper electrodes is exemplified in Figure 1A. FDM 3D printer (Adventurer 4, FlashForge, China) printed a rectangular plate (20 mm width × 10 mm height × 3 mm depth) using the Acccreate filament, based on copper particles and PLA. The printer was equipped with a 0.6 mm printing nozzle. The printing parameters were 220 °C nozzle temperature, 60 °C bed temperature, 65 mm s^{-1} printing speed, 0.1 mm layer height, and 100% infill. The working electrodes (WEs) were sintered with a Work Special Laser machine. The optimum processing conditions were 1.6 W laser power, 5 mm s^{-1} scan rate, 12 mm height (distance between the laser output and the printed substrate), and 0.1750 mm distance between the laser-engraved beamlines. The electrical conductivity of the resulting materials was initially tested with a LED lamp connected to a 4.5 V battery. Subsequently, they were characterized by cyclic voltammetry using a 5 mL electrochemical cell. The working electrode area was delimited using a hot glue gun.

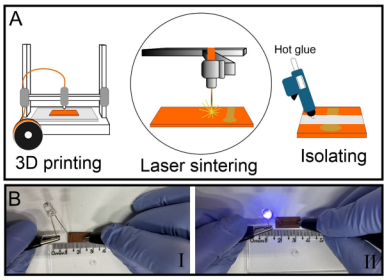

Figure 1. (A) Fabrication process of copper electrodes using 3D printing and laser sintering. (B) A conductivity test was performed on the printed plate (I) before and (II) after laser sintering. This test was conducted with an LED lamp connected to a 4.5 V battery.

The electrochemical experiments were performed with an Autolab PGSTAT128N potentiostat/galvanostat (Eco Chemie, Utrecht, The Netherlands) connected to a microcomputer managed by the NOVA 2.1.7 software. The measurements were conducted with the resulting copper electrode as the working electrode, a platinum wire as the counter electrode, and Ag/AgCl/KCl_{sat} as the reference electrode. The copper electrodes were initially characterized by cyclic voltammetry. Subsequently, amperometry was used to evaluate laser processing parameters considering the sensor sensitivity for glucose quantification.

The scanning electron microscopy (SEM) images were obtained with a JEOL JSM-7401F microscope. Elemental analysis was carried out by energy-dispersive X-ray spectroscopy (EDS). Contact angle determination was conducted by dropping an aliquot of 10 μL of water on the substrate surface, followed by image capture with a VEDO VD3035s digital optical microscope. The angles were then measured with the ImageJ software. Raman spectra were acquired using a Renishaw InVia Raman microscope equipped with a CCD detector and coupled to an Olympus BHT2 microscope. A 20x long working distance Olympus objective and a 532 nm laser (Renishaw) were used for excitation. Spectra were collected

https://doi.org/10.1021/acsaelm.5c00862
ACS Appl. Electron. Mater. XXXX, XXX, XXX−XXX

with a laser power of 1 mW, using two accumulations of 20 s each.

2.3. Copper Quantification in the Acccreate Filament. The copper quantification was performed by weighing 0.2218 g of filament, followed by its dissolution in 2 mL of concentrated nitric acid using sonication. Ten μL of the resulting solution was added to an electrochemical cell containing 10 mL of acetate buffer solution. The electrochemical measurements were conducted with differential pulse voltammetry using a gold electrode as a working electrode, Ag/AgCl/KCl_{sat} as the reference electrode, and a platinum wire as the counter electrode. After recording the sample measurement, successive additions of copper standard solution were added to the solution, enabling the copper quantification by the standard addition method.

2.4. Oral Rehydration Sample Analyses. The glucose in oral rehydration samples was quantified using the standard addition method. The experiments consisted of recording amperometric measurements in 5 mL of KOH 0.1 mol L^{-1} at +0.6 V vs Ag/AgCl/KCl_{sat}. After starting the measurements, an aliquot of an oral rehydration sample (45 μL of hidroral, 22 μL of Hydraplex, and 18.5 μL of Rehidrate) was added to 5 mL of KOH 0.1 mol L^{-1}, followed by the addition of standard glucose solutions. This study was conducted in triplicate. The addition of sample and standard solutions to the supporting electrolyte solution promoted an increase in the amperometric currents, resulting in a graph with a stair-step format. The respective current intensities were then used to plot the calibration curves. Subsequently, the glucose concentration present in the sample was calculated using the respective equations of the calibration curves, extrapolating the curve to the *y*-axis equal to zero. The oral rehydration solution contains a mixture of potassium chloride, sodium citrate, sodium chloride, and glucose. According to the manufacturer, the glucose concentration levels are 20.0 g L^{-1} for Hidroral, 20.0 g L^{-1} for Hidraplex, and 24.1 g L^{-1} for Rehidrat.

3. RESULTS AND DISCUSSION

3.1. Characterization Studies of Copper Electrodes. To evaluate the ability to sinter the 3D-printed parts using a laser engraving machine, a simple test (Figure 1B) was initially conducted with sintered and nonsintered materials, utilizing an LED lamp connected to a 4.5 V battery. This test indicates that the laser irradiation changed the material properties, resulting in a conductive surface after the laser sintering process. Electrical conductivity gain (Figure 1B) is evident when an LED lamp is connected in the laser-processed area. This conductive surface formation could be associated with the photothermal reduction of metal ions on the substrates, which occurs when the infrared (IR) laser beam is directly irradiated on the substrate, reaching high local temperatures (>2500 °C, depending on the laser power).[14,15,27]

Next, the substrate hydrophobicity was evaluated by contact angle determination (Figure S1). The contact angle was (110 ± 0.4)° for the nonsintered surface and (136.4 ± 0.4)° for the sintered copper plate, demonstrating that the hydrophobicity increased after laser sintering. The materials were also characterized by Raman spectroscopy. A Raman spectrum characteristic of the PLA matrix is observed for the nonsintered surface (Figure S2).[28] The spectrum shows strong bands in the range of 3100−2800 cm^{-1}. These bands correspond to C−H stretching modes of $-CH_3$ and $-CH_2-$. The band at 1455 cm^{-1} is associated with the CH_3 deformation, and the band at 873 cm^{-1} is attributed to the C−COO stretching of the repeated polymer unit. Raman spectrum (Figure S2) was also recorded for the laser-sintered material, showing an additional prominent band at 1593 cm^{-1}. This is likely associated with sp^2 carbon hybridization generated after laser sintering.[29] The presence of these unsaturated groups (C═C) contributes to the increase of the material hydrophobicity, agreeing with the results observed by contact angle determination.

Next, scanning electron microscopy (SEM) images were recorded before and after laser sintering. The morphological aspects of the printed material remarkably changed after laser processing (Figure 2A). Along with the morphological changes, the copper content on the resulting sintered surface significantly increased, as further documented by the color elemental mapping images of copper (Figure 2), indicating that the laser beam promoted the formation of metallic copper. No significant difference was observed in the color elemental mapping images of carbon and oxygen (Figure S3), likely due to their high quantities in the PLA matrix. The EDS spectra (Figure S4) confirm the presence of each element. Additionally, the spectra provide the weight percentages of each component, demonstrating that the copper content present in the sintered surface increased from 16.25% to 36.65%, which justifies the enhancement of the conductive properties of the printed material after laser processing.

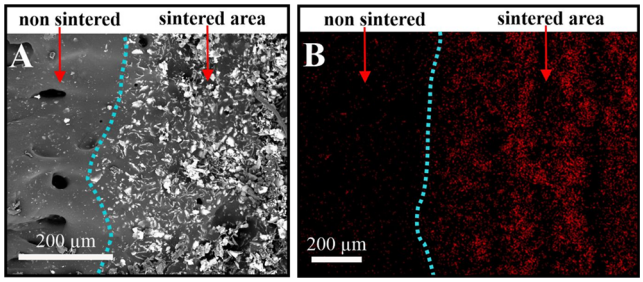

Figure 2. Morphological characterizations recorded for nonsintered and sintered regions. (A) SEM micrograph of the printed material and (B) color elemental mapping images of copper.

According to the manufacturer, the filament is based on a PLA plastic matrix embedded with copper particles, which presents no conductive properties in its current form. The copper content is not disclosed, likely due to commercial confidentiality. Considering this, the copper quantity was further determined by the standard addition method using differential pulse voltammetry (Figure S5), with the resulting value corresponding to 13.5% in mass. This percentage is close to the values estimated through color elemental mapping images (16.25%), suggesting a uniform copper distribution in the filament. Besides the uniformity, commercial conductive filaments typically contain a low percentage of conductive materials to prevent printing errors,[30] such as filament breaking and printing nozzle clogging.

After evaluating the electrical and morphological properties, the sintered electrode was characterized by cyclic voltammetry. Figure 3A shows that the resulting electrode has a voltammetric profile comparable to that obtained with a copper wire electrode, indicating the presence of copper metal particles in the metal-filled filament. The voltammogram of the sintered electrodes also showed a small oxidation peak at −0.5 V, potentially generated by some species present in the filament that stabilize one of the Cu(I) processes, eq 1. Such

https://doi.org/10.1021/acsaelm.5c00862
ACS Appl. Electron. Mater. XXXX, XXX, XXX−XXX

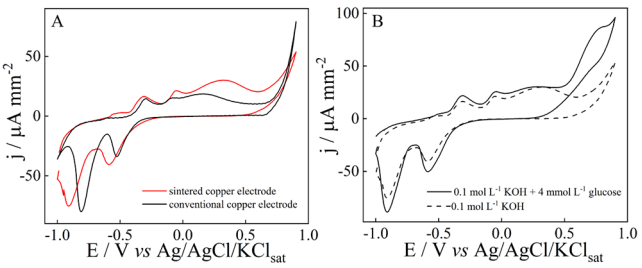

Figure 3. (A) Cyclic voltammograms were recorded with a copper wire electrode and the sintered 3D-printed copper electrode. (B) Cyclic voltammograms were recorded with the sintered copper electrode in the absence and presence of 4 mmol L^{-1} glucose. Supporting electrolyte: 0.1 mol L^{-1} KOH. Scan rate: 50 mV s^{-1}.

stabilization is often facilitated by ligands capable of forming thermodynamically stable complexes. The precise anodic potential at which these species are oxidized can be influenced by a range of factors, including local pH, the nature of the coordinating environment, and the extent of chemical oxidation,[31] which contribute to the variable electrochemical behavior of copper species.

$$2Cu + 2OH^- \rightleftharpoons Cu_2O + H_2O + 2e^- \quad (1)$$

Figure 3A also exhibits a voltammetric peak of Cu to Cu(I) oxidation at approximately −0.4 V.[32−34] Two other peaks are observed between −0.1 and +0.4 V. These peaks correspond to the oxidation of Cu(I) to Cu(II), forming oxide and hydroxide species as exemplified by eqs 2−6.[32−34]

$$Cu + 4OH^- \rightleftharpoons Cu(OH)_4^{2-} + 2e^- \quad (2)$$

$$Cu_2O + 6OH^- + H_2O \rightleftharpoons 2Cu(OH)_4^{2-} + 2e^- \quad (3)$$

$$Cu_2O + 2OH^- + H_2O \rightleftharpoons 2Cu(OH)_2 + 2e^- \quad (4)$$

$$Cu + 2OH^- \rightleftharpoons Cu(OH)_2 + 2e^- \quad (5)$$

$$Cu + 2OH^- \rightleftharpoons CuO + H_2O + 2e^- \quad (6)$$

Besides copper characteristic behavior, cyclic voltammograms (Figure 3B) were also recorded in the presence of 4 mmol L^{-1} of glucose, demonstrating that glucose is oxidized at the sintered copper electrode surface. The glucose oxidation mechanism is not clearly understood,[23,35,36] with some works[23,35] reporting that Cu(III) from the copper electrode surface mediates (Figure S6) the oxidation process of sugars, such as glucose. This oxidation mechanism involves the electrochemical oxidation of a layer of copper(II) oxides and hydroxides to CuOOH, which catalyzes glucose oxidation through a chemical reaction.[37,38] Other studies proposed that Cu(III) species do not contribute to the oxidation mechanism of carbohydrates. Instead, hydroxyl ion adsorption and the semiconductive properties of the material play a more dominant role in this process.[36] Regardless of the mechanism, the proposed copper electrodes showed promising results for glucose quantification, demonstrating potential utility in analytical applications.

The subsequent study evaluated the glucose amperometric response under different potentials (Figure 4A). The amperograms (Figure 4A) show the current increase with successive additions of glucose standard solutions, resulting in a graphic with a stair format. Analytical curves (Figure 4B) were plotted with the current magnitude obtained after successive injections. The sensitivity increases upon increasing the potential up to +0.7 V, reaching a plateau. Even though +0.7 V provided the highest sensitivity, the sensors showed low signal stabilization during subsequent additions of standard glucose solutions. This behavior is likely due to undesirable parallel reactions, such as solvent oxidation, affecting the sensor response. This effect is even more evident when +0.8 V is applied, generating high noise in the background current, probably because of the oxygen bubbles that form during water oxidation. Considering that, + 0.6 V was the detection potential for the laser processing studies, described in the next section.

3.2. Laser Processing Optimization of Copper Electrodes. Laser power was the first parameter assessed, with the amperograms and respective calibration curves shown in Figure 5A,B. <1.4W power was not enough to form a conductive film. In contrast, the film was formed by varying the laser power between 1.4 and 2.0W, resulting in equal sensor sensitivity (Figure 5C) under these processing conditions. This indicates that the copper film can be effectively formed with this range of laser power. This laser power demand is within the values necessary for copper ink sintering on polycarbonate substrates,[13] with power values ranging from 1.5 to 5 W. In the present study, >2.0W laser power caused substrate overheating, damaging the printed material, and restricting the electrode use. Considering this result, 1.6 W laser power was selected to study the laser scan rate.

The amperograms and respective calibration curves of electrodes sintered under different laser scan rates are shown in Figures S7A and S7B. Figure 5D shows that the laser scan rate remarkably changed the sensor sensitivity upon varying

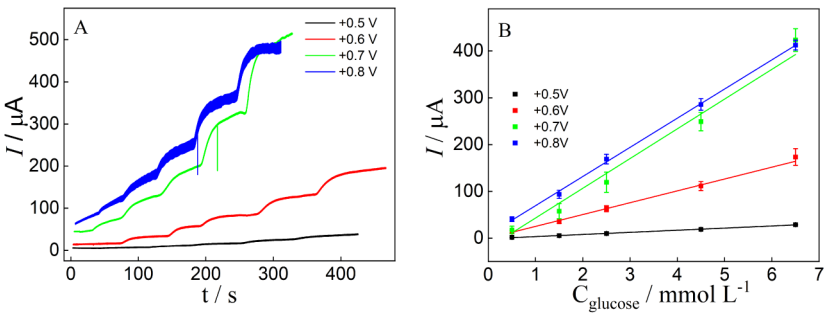

Figure 4. Influence of the detection potential on sensor response for glucose oxidation. (A) Amperograms and (B) respective calibration curves of sintered copper electrodes recorded with successive injections of glucose standard solutions from +0.5 to +0.8 V vs Ag/AgCl/KCl_{sat}. Supporting electrolyte: 0.1 mol L^{-1} KOH. Error bars represent the standard deviation of three independent electrodes.

https://doi.org/10.1021/acsaelm.5c00862
ACS Appl. Electron. Mater. XXXX, XXX, XXX−XXX

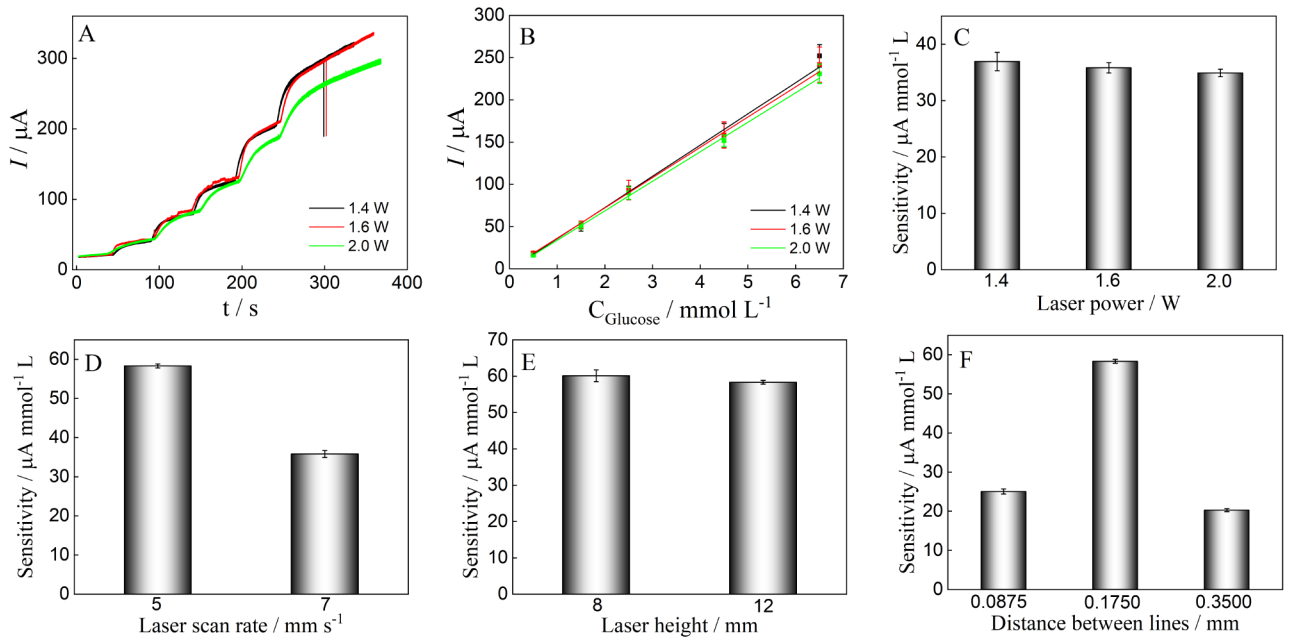

Figure 5. Evaluation of the laser processing parameters using sensor response for glucose oxidation: (A) Amperograms and (B) respective calibration curves recorded with sintered copper electrodes with successive injections of glucose standard solutions. Supporting electrolyte: 0.1 mol L^{-1} KOH. Detection potential: + 0.6 V vs $Ag/AgCl/KCl_{sat}$. Influence of the (C) laser power, (D) laser scan rate, (E) laser height, and (F) distance between the laser lines on the sensor sensitivity for glucose oxidation. Error bars represent the standard deviation of three independent electrodes.

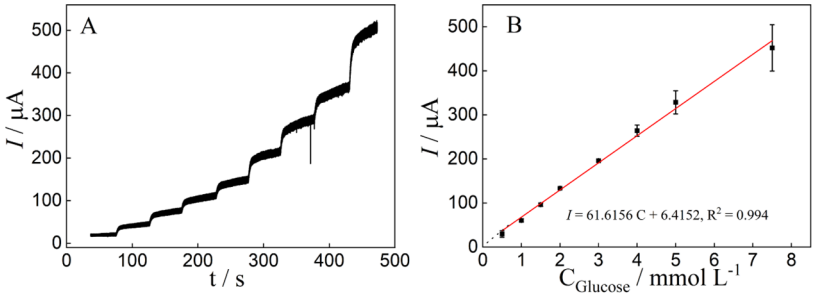

Figure 6. Linear range for glucose was evaluated with sintered copper electrodes. (A) amperograms recorded with sintered copper electrodes with successive injections of glucose standard solutions. Supporting electrolyte: 0.1 mol L-1 KOH. Detection potential: + 0.6 V vs Ag/AgCl/KClsat. (B) Analytical curve for glucose.

the values from 5 to 7 mm s^{-1}. Five mm s^{-1} yielded higher sensitivity, suggesting that a more conductive copper film is formed by slowly scanning the laser beam.[39] Next, the height between the laser output and the printed substrate was evaluated in this study. Figures S8A and S8B show the amperograms and respective calibration curves. Even though defocusing the laser beam (focal length = 12 mm) could potentially decrease the local heating by widening the laser spot's size,[40] the laser height showed no significant difference in sensitivity (Figure 5E). Therefore, 12 mm height was selected as the optimum condition.

Finally, the distance between the laser beamlines was evaluated. Figures S9A and S9B show the amperograms and respective analytical plots. Depending on the processing condition, the laser beam scanning can overlap the laser lines or leave a gap between them (known as a scan gap).[40,41] <0.0875 mm lines damaged the substrate surface because of the overlapping of engraved lines, causing substrate overheating. In contrast, the sensitivity (Figure 5F) increased with the distance from 0.0875 to 0.1750 mm, likely due to the more uniform surface at a distance of 0.1750 mm, resulting in a copper film with higher electrical conductivity. Despite that, the sensitivity decreased upon changing the line distance to 0.3500 mm. This behavior is attributed to the reduced number of individual engraved lines formed per unit of area when the distance between lines is increased, resulting in a lower electrical conductivity. Considering this result, subsequent studies were conducted with a line distance of 0.1750 mm.

3.3. Analytical Applicability of Copper Electrodes for Glucose Quantification. Under optimum conditions, the fabrication reproducibility was evaluated with three different sensors (Figure S10A), demonstrating they provided a consistent amperometric response (Figure S10B) with a relative standard deviation (RSD) of only 3% for sensitivity values. Also, the sensor response (Figure 6A) was evaluated by amperometry from 0.5 to 7.5 mmol L^{-1} glucose, with the linearity (Figure 6B) represented by the following equation: I (μA) = 61.6 C + 6.42, R^2 = 0.994. The limits of detection (LOD) and quantification (LOQ) were 0.045 and 0.15 mmol L^{-1}, respectively. The merit figures were calculated by the following equations: LOD = 3 Sd (blank)/m and LOQ = 10 Sd (blank)/m. Sd (blank) is the standard deviation of the

https://doi.org/10.1021/acsaelm.5c00862
ACS Appl. Electron. Mater. XXXX, XXX, XXX−XXX

blank (0.9199), and m corresponds to the slope of the analytical curve (61.6156).

Next, the sensor's applicability was evaluated for analyzing oral rehydration solutions. Such samples are essential in managing dehydration, which is primarily caused by diarrhea and vomiting. The labeled sample composition includes potassium chloride, sodium citrate, sodium chloride, and glucose. The glucose quantification was performed using the standard addition method (Figure S11), with the results summarized in Table 1. A *t* test was applied to compare the

Table 1. Glucose Quantification in Oral Rehydration Solution Samples

Sample	Labeled concentration/ g L^{-1}	[a]Found concentration g L^{-1}	[b]*t* test
Hidroral	20.0	15 ± 4	2.34
Hidraplex	20.0	22 ± 4	0.63
Rehidrat	24.1	23 ± 3	0.59

[a]Values expressed as average ± SD. [b]$T_{critical}$ with 95% confidence level = 4.3 (n − 1 = 2 degrees of freedom).

result with the informed values, resulting in $t_{calculated} < t_{critical}$ values. The results indicated that the proposed method offers accuracy for glucose quantification, providing results statistically equivalent (95% confidence level) to the values informed by the manufacturer. Subsequently, the sensor selectivity was assessed for glucose oxidation (Figures S12 and S13). This study was conducted by adding glucose and possible interfering species, including nitrite, sulfite, caffeine, ascorbic acid, maltose, saccharose, creatinine, and uric acid.[42] Among them, ascorbic acid, sulfite, uric acid, and creatinine changed the sensor response, indicating they could affect the glucose analytical signal. Consequently, the proposed method is restricted to the analysis of samples containing these compounds. Despite that, the proposed sensors were directly used for oral rehydration solution sample analyses without any additional step, with the results (Table 1) showing that the sample matrices had no significant effect on the sensor responses. Additionally, the analytical parameters of the proposed method for glucose quantification were compared with those of other recent methods, as shown in Table 2. The linear range of the sintered copper electrodes is compatible with those of other nonenzymatic electrodes. Although some sensors demonstrated better detection limit (LOD), glucose concentrations in drink samples are typically high, eliminating the need for low-detectability sensors. Unlike previously reported sensors, the proposed electrodes are disposable, and their fabrication process is scalable. Furthermore, the fabrication does not require additional chemical components for surface modification, allowing the electrodes to be used immediately after fabrication. Moreover, the laser sintering process enables the patterning of conductive lines in various sizes and geometries, facilitating the miniaturization of analytical systems. Therefore, the simplicity and scalability of the proposed electrode fabrication method offer notable advantages and represent a promising advancement in the development of disposable sensors for (bio)analytical applications.

4. CONCLUSIONS

This work combined 3D printing and laser sintering to fabricate disposable copper electrodes. The laser source produced copper films on the nonconductive surface of the printed material, providing electrical conductivity to the resulting sensors. The laser processing parameters affected the sensor sensitivity for glucose oxidation, with the optimal parameters being 1.6W laser power, 5 mm s^{-1} scan rate, 12 mm height, and 0.1750 mm line distance. Unlike conventional processes for fabricating conductive films, our method does not rely on expensive instrumentation. Compared to thermal sintering, the proposed laser sintering method showed rapidness and the potential utility for patterning different designs, increasing the sensor's versatility. Additionally, the sensors can be readily used after fabrication, eliminating the need for further processing. Therefore, this work brings a novel alternative for copper electrode fabrication, offering scalability

Table 2. Comparison of the Analytical Parameter of the Copper Electrodes for Glucose Quantification with Previous Works[a]

Electrode	Technique	Linear range/mmol L^{-1}	LOD/mmol L^{-1}	Reference
Pd−Cu BMA/SPE	Amperometry	1−20	0.043	43
CNQDs/PANI	Cyclic voltammetry	0.05−0.5	0.029	44
CuS/rGO/Gox/GCE	LSV	0.1−100	1.75×10^{-6}	45
Cu_2O/PET electrode	Amperometry	0.01−18	0.002	46
Copper 3D electrode	Cyclic voltammetry	0.001−0.050	6×10^{-5}	9
$CuFe_2O_4$/S-GO/G/SPE	LSV	0.0075−0.1	0.003	47
QSM/Au/Ni/CFME	Amperometry	0.05−16.2	11.3×10^{-3}	48
XSBR-PEDOT:PSS-AMWCNTs/AuNPs/SPE	Amperometry	0.05−0.6	3.2×10^{-3}	48
Ag@TiO2/TP	Amperometry	0.001−4	0.18×10^{-3}	49
NiO/SPE	Amperometry	0.1−0.7	0.25×10^{-3}	50
Ni@CoxSy/PEDOT rGO	Amperometry	0.0002−2.0	0.094×10^{-3}	51
Sintered copper electrodes	Amperometry	0.5 − 7.5	0.045	This work

[a]Pd−Cu BMA/SPE: Palladium−copper bimetallic aerogels/screen-printed electrode. CNQDs/PANI: Carbon Nitride Quantum Dots/Polyaniline Nanocomposites. LSV: Linear sweep voltammetry. CuS/rGO/Gox/GCE: Copper sulfate/Reduced graphene oxide/Glucose oxidase/Glassy carbon electrodes. Copper 3D electrodes: 3D printed copper electrodes sintered in a tubular furnace. $CuFe_2O_4$/S-GO/G/SPE: copper ferrite/sulfur-doped graphene oxide/graphite/screen-printed electrode. QSM: biopolymer layer derived from quince seed mucilage. CFME: carbon fiber microelectrodes. XSBR: Carboxylated styrene butadiene rubber. PEDOT:PSS: Poly(3,4-ethylenedioxythiophene): Poly(styrenesulfonate). AMWCNTs: aminated multiwalled carbon nanotubes. AuNPs: gold nanoparticles. Ag@TiO_2/TP: Silver nanoparticle-decorated titanium dioxide nanoribbon array on titanium plate. NiO: nickel oxide. Ni@CoxSy/PEDOT rGO: ternary hierarchical hybrid Ni@CoxSy/poly(3,4-ethylenedioxythiophene)-reduced graphene oxide.

https://doi.org/10.1021/acsaelm.5c00862
ACS Appl. Electron. Mater. XXXX, XXX, XXX−XXX

and possibilities for sensing applications beyond glucose quantification.

■ ASSOCIATED CONTENT

Supporting Information

The Supporting Information is available free of charge at https://pubs.acs.org/doi/10.1021/acsaelm.5c00862.

Scheme of glucose oxidation process at the copper electrode surface, evaluation of the laser processing parameters, graphics of copper quantification in the filament using the standard addition method with differential pulse voltammetry, reproducibility and selectivity studies, and graphics of the analyses of oral rehydration samples (PDF)

■ AUTHOR INFORMATION

Corresponding Authors

Lauro A. Pradela-Filho − *Institute of Chemistry, Department of Fundamental Chemistry, University of São Paulo, São Paulo, SP 05508-000, Brazil;* orcid.org/0000-0002-0468-1953; Email: lauropradela@usp.br

Thiago R. L. C. Paixão − *Institute of Chemistry, Department of Fundamental Chemistry, University of São Paulo, São Paulo, SP 05508-000, Brazil;* orcid.org/0000-0003-0375-4513; Email: trlcp@iq.usp.br

Authors

Priscila S. L. Silva − *Institute of Chemistry, Department of Fundamental Chemistry, University of São Paulo, São Paulo, SP 05508-000, Brazil;* orcid.org/0009-0003-4662-2972

Diele A. G. Araujo − *Institute of Chemistry, Department of Fundamental Chemistry, University of São Paulo, São Paulo, SP 05508-000, Brazil;* orcid.org/0000-0002-9089-8701

Débora N. Medeiros − *Institute of Chemistry, Department of Fundamental Chemistry, University of São Paulo, São Paulo, SP 05508-000, Brazil;* orcid.org/0000-0001-7105-5824

Rômulo A. Ando − *Institute of Chemistry, Department of Fundamental Chemistry, University of São Paulo, São Paulo, SP 05508-000, Brazil;* orcid.org/0000-0002-3872-8094

Complete contact information is available at: https://pubs.acs.org/10.1021/acsaelm.5c00862

Author Contributions

The manuscript was written through the contributions of all authors. All authors have approved the final version of the manuscript.

Funding

The Article Processing Charge for the publication of this research was funded by the Coordenacao de Aperfeicoamento de Pessoal de Nivel Superior (CAPES), Brazil (ROR identifier: 00x0ma614).

Notes

The authors declare no competing financial interest.

■ ACKNOWLEDGMENTS

The authors are grateful to Coordenação de Aperfeiçoamento de Pessoal de Nível Superior − Brasil (CAPES) − Finance Code 001, São Paulo Research Foundation - FAPESP (2022/11346-4, 2022/01810-5, 2021/00205-8, 2018/08782-1, and 2023/00246-1), Conselho Nacional de Desenvolvimento Científico e Tecnológico − CNPq (311847-2018-8, 302839/2020-8, 405620/2021-7), and Instituto Nacional de Ciência e Tecnologia de Bioanalítica − INCTBio (302839/2020-8) for the financial support. The authors also thank Prof. Gabriel Meloni for the helpful discussions regarding SEM characterization.

■ REFERENCES

(1) Xie, L.; Abliz, D.; Li, D. Thin Film Coating for Polymeric Micro Parts. *Compr. Mater. Process. Thirteen Vol. Set.* **2014**, *7*, 157−170.

(2) Sun, L.; Yuan, G.; Gao, L.; Yang, J.; Chhowalla, M.; Gharahcheshmeh, M. H.; Gleason, K. K.; Choi, Y. S.; Hong, B. H.; Liu, Z. Chemical Vapour Deposition. *Nat. Rev. Methods Prim.* **2021**, *1* (1), 5.

(3) Zamani, M.; Klapperich, C. M.; Furst, A. L. Recent Advances in Gold Electrode Fabrication for Low-Resource Setting Biosensing. *Lab Chip.* **2023**, *23* (5), 1410−1419.

(4) Berkheimer, Z. A.; Tahir, A.; Nordin, G. P.; Paixão, T. R. L. C.; Woolley, A. T.; Do Nascimento, G. H. M.; de Araujo, W. R.; Pradela-Filho, L. A. Extruded Filament Electrodes for Lactate Biosensing in Continuous-Injection Paper-Based Microfluidic Devices. *Biosens. Bioelectron.* **2025**, *278*, 117390.

(5) Pradela-Filho, L. A.; Veloso, W. B.; Medeiros, D. N.; Lins, R. S. O.; Ferreira, B.; Bertotti, M.; Paixão, T. R. L. C. Patterning (Electro)Chemical Treatment-Free Electrodes with a 3D Printing Pen. *Anal. Chem.* **2023**, *95* (28), 10634−10643.

(6) Pradela-Filho, L. A.; Araújo, D. A. G.; Ataide, V. N.; Meloni, G. N.; Paixão, T. R. L. C. Challenges Faced with 3D-Printed Electrochemical Sensors in Analytical Applications. *Anal. Bioanal. Chem.* **2024**, *416*, 4679.

(7) Veloso, W. B.; Paixão, T. R. L. C.; Meloni, G. N. The Current Shortcomings and Future Possibilities of 3D Printed Electrodes. *Anal. Chem.* **2024**, *96*, 14315−14319.

(8) Flowers, P. F.; Reyes, C.; Ye, S.; Kim, M. J.; Wiley, B. J. 3D Printing Electronic Components and Circuits with Conductive Thermoplastic Filament. *Addit. Manuf.* **2017**, *18* (2017), 156−163.

(9) Redondo, E.; Pumera, M. Fully Metallic Copper 3D-Printed Electrodes via Sintering for Electrocatalytic Biosensing. *Appl. Mater. Today* **2021**, *25*, 101253.

(10) Redondo, E.; Ng, S.; Muñoz, J.; Pumera, M. Tailoring Capacitance of 3D-Printed Graphene Electrodes by Carbonisation Temperature. *Nanoscale* **2020**, *12* (38), 19673−19680.

(11) Lin, J.; Peng, Z.; Liu, Y.; Ruiz-Zepeda, F.; Ye, R.; Samuel, E. L. G.; Yacaman, M. J.; Yakobson, B. I.; Tour, J. M. Laser-Induced Porous Graphene Films from Commercial Polymers. *Nat. Commun.* **2014**, *5*, 5.

(12) Rocha, D. P.; Ataide, V. N.; de Siervo, A.; Gonçalves, J. M.; Muñoz, R. A. A.; Paixão, T. R. L. C.; Angnes, L. Reagentless and Sub-Minute Laser-Scribing Treatment to Produce Enhanced Disposable Electrochemical Sensors via Additive Manufacture. *Chem. Eng. J.* **2021**, *425*, 130594.

(13) Peng, P.; Li, L.; He, P.; Zhu, Y.; Fu, J.; Huang, Y.; Guo, W. One-Step Selective Laser Patterning of Copper/Graphene Flexible Electrodes. *Nanotechnology* **2019**, *30* (18), 185301.

(14) Arantes, I. V. S.; Ataide, V. N.; Ameku, W. A.; Gongoni, J. L. M.; Selva, J. S. G.; Nogueira, H. P.; Bertotti, M.; Paixão, T. R. L. C. Laser-Induced Fabrication of Gold Nanoparticles onto Paper Substrates and Their Application on Paper-Based Electroanalytical Devices. *Sens. Diagn.* **2023**, *2* (1), 111−121.

(15) Veloso, W. B.; Meloni, G. N.; Arantes, I. V. S.; Pradela-Filho, L. A.; Muñoz, R. A. A.; Paixão, T. R. L. C. Gold Film Deposition by Infrared Laser Photothermal Treatment on 3D-Printed Electrodes: Electrochemical Performance Enhancement and Application. *Analyst* **2024**, *149* (15), 3900.

(16) Scroccarello, A.; Álvarez-Diduk, R.; Della Pelle, F.; de Carvalho Castro e Silva, C.; Idili, A.; Parolo, C.; Compagnone, D.; Merkoçi, A. One-Step Laser Nanostructuration of Reduced Graphene Oxide Films Embedding Metal Nanoparticles for Sensing Applications. *ACS Sens.* **2023**, *8* (2), 598−609.

(17) Kuwahara, T.; Ogawa, K.; Sumita, D.; Kondo, M.; Shimomura, M. Amperometric Glucose Sensing with Polyaniline/Poly(Acrylic Acid) Composite Film Bearing Glucose Oxidase and Catalase Based on Competitive Oxygen Consumption Reactions. *J. Electroanal. Chem.* **2018**, *811*, 62−67.
(18) Cardoso, R. M.; Silva, P. R. L.; Lima, A. P.; Rocha, D. P.; Oliveira, T. C.; Do Prado, T. M.; Fava, E. L.; Fatibello-Filho, O.; Richter, E. M.; Muñoz, R. A. A. 3D-Printed Graphene/Polylactic Acid Electrode for Bioanalysis: Biosensing of Glucose and Simultaneous Determination of Uric Acid and Nitrite in Biological Fluids. *Sens. Actuators, B* **2020**, *307*, 127621.
(19) Blasques, R. V.; Stefano, J. S.; Camargo, J. R.; Guterres e Silva, L. R.; Brazaca, L. C.; Janegitz, B. C. Disposable Prussian Blue-Anchored Electrochemical Sensor for Enzymatic and Non-Enzymatic Multi-Analyte Detection. *Sens. Actuators Rep.* **2022**, *4*, 100118.
(20) Kalinke, C.; Wosgrau, V.; Oliveira, P. R.; Oliveira, G. A.; Martins, G.; Mangrich, A. S.; Bergamini, M. F.; Marcolino-Junior, L. H. Green Method for Glucose Determination Using Microfluidic Device with a Non-Enzymatic Sensor Based on Nickel Oxyhydroxide Supported at Activated Biochar. *Talanta* **2019**, *200*, 518−525.
(21) Ling, P.; Zhang, Q.; Cao, T.; Gao, F. Versatile Three-Dimensional Porous Cu@Cu 2 O Aerogel Networks as Electrocatalysts and Mimicking Peroxidases. *Angew. Chem., Int. Ed.* **2018**, *57* (23), 6819−6824.
(22) Bessant, C.; Saini, S. Simultaneous Determination of Ethanol, Fructose, and Glucose at an Unmodified Platinum Electrode Using Artificial Neural Networks. *Anal. Chem.* **1999**, *71* (14), 2806−2813.
(23) Kumar, K. P. A.; Ghosh, K.; Alduhaish, O.; Pumera, M. Metal-Plated 3D-Printed Electrode for Electrochemical Detection of Carbohydrates. *Electrochem. Commun.* **2020**, *120*, 106827.
(24) Grujicic, D.; Pesic, B. Electrodeposition of Copper: The Nucleation Mechanisms. *Electrochim. Acta* **2002**, *47* (18), 2901−2912.
(25) Zen, J.-M.; Hsu, C.-T.; Kumar, A. S.; Lyuu, H.-J.; Lin, K.-Y. Amino Acid Analysis Using Disposable Copper Nanoparticle Plated Electrodes. *Analyst* **2004**, *129* (9), 841−845.
(26) Novakowski, W.; Bertotti, M.; Paixão, T. R. L. C. Use of Copper and Gold Electrodes as Sensitive Elements for Fabrication of an Electronic Tongue: Discrimination of Wines and Whiskies. *Microchem. J.* **2011**, *99* (1), 145−151.
(27) Mendes, L. F.; de Siervo, A.; Reis de Araujo, W.; Longo Cesar Paixão, T. R. Reagentless Fabrication of a Porous Graphene-like Electrochemical Device from Phenolic Paper Using Laser-Scribing. *Carbon* **2020**, *159*, 110−118.
(28) Vano-Herrera, K.; Misiun, A.; Vogt, C. Preparation and Characterization of Poly(Lactic Acid)/Poly(Methyl Methacrylate) Blend Tablets for Application in Quantitative Analysis by Micro Raman Spectroscopy. *J. Raman Spectrosc.* **2015**, *46* (2), 273−279.
(29) Cardoso, R. M.; Rocha, D. P.; Rocha, R. G.; Stefano, J. S.; Silva, R. A. B.; Richter, E. M.; Muñoz, R. A. A. 3D-Printing Pen versus Desktop 3D-Printers: Fabrication of Carbon Black/Polylactic Acid Electrodes for Single-Drop Detection of 2,4,6-Trinitrotoluene. *Anal. Chim. Acta* **2020**, *1132* (1132), 10−19.
(30) Stefano, J. S.; Kalinke, C.; Da Rocha, R. G.; Rocha, D. P.; Da Silva, V. A. O. P.; Bonacin, J. A.; Angnes, L.; Richter, E. M.; Janegitz, B. C.; Muñoz, R. A. A. Electrochemical (Bio)Sensors Enabled by Fused Deposition Modeling-Based 3D Printing: A Guide to Selecting Designs, Printing Parameters, and Post-Treatment Protocols. *Anal. Chem.* **2022**, *94* (17), 6417−6429.
(31) Kok, J.; de Ruiter, J.; van der Stam, W.; Burdyny, T. Interrogation of Oxidative Pulsed Methods for the Stabilization of Copper Electrodes for CO2 Electrolysis. *J. Am. Chem. Soc.* **2024**, *146*, 19509.
(32) Dantas, L. M. F.; DeSouza, A. P. R.; Castro, P. S.; Paixão, T. R. L. C.; Bertotti, M. SECM Studies on the Electrocatalytic Oxidation of Glycerol at Copper Electrodes in Alkaline Medium. *Electroanalysis* **2012**, *24* (8), 1778−1782.
(33) Paixão, T. R. L. C.; Ponzio, E. A.; Torresi, R. M.; Bertotti, M. EQCM Behavior of Copper Anodes in Alkaline Medium and Characterization of the Electrocatalysis of Ethanol Oxidation by Cu(III). *J. Braz. Chem. Soc.* **2006**, *17* (2), 374−381.
(34) Paixão, T. R. L. C.; Bertotti, M. Development of a Breath Alcohol Sensor Using a Copper Electrode in an Alkaline Medium. *J. Electroanal. Chem.* **2004**, *571* (1), 101−109.
(35) Aun, A. T. T.; Salleh, N. M.; Ali, U. F. M.; Basirun, W. J.; Chang, Y.-H.; Manan, N. S. A. Renewable Non-Enzymatic Copper-Based Surfaces for the Detection of Glucose, Fructose, Sucrose, and Galactose. *J. Food Compos. Anal.* **2025**, *139*, 107119.
(36) Barragan, J. T. C.; Kogikoski, S.; Da Silva, E. T. S. G.; Kubota, L. T. Insight into the Electro-Oxidation Mechanism of Glucose and Other Carbohydrates by CuO-Based Electrodes. *Anal. Chem.* **2018**, *90* (5), 3357−3365.
(37) Huang, T. K.; Lin, K. W.; Tung, S. P.; Cheng, T. M.; Chang, I. C.; Hsieh, Y. Z.; Lee, C. Y.; Chiu, H. T. Glucose Sensing by Electrochemically Grown Copper Nanobelt Electrode. *J. Electroanal. Chem.* **2009**, *636* (1−2), 123−127.
(38) Paixão, T. R. L. C.; Corbo, D.; Bertotti, M. Amperometric Determination of Ethanol in Beverages at Copper Electrodes in Alkaline Medium. *Anal. Chim. Acta* **2002**, *472* (1−2), 123−131.
(39) Gongoni, J. L. M.; Filho, L. A. P.; De Farias, D. M.; Arantes, I. V. S.; Paixão, T. R. L. C. Modulating the Electrochemical Response of Eco-Friendly Laser-Pyrolyzed Paper Sensors Applied to Nitrite Determination. *ChemElectrochem* **2023**, *10* (1), No. e202201018.
(40) Chyan, Y.; Ye, R.; Li, Y.; Singh, S. P.; Arnusch, C. J.; Tour, J. M. Laser-Induced Graphene by Multiple Lasing: Toward Electronics on Cloth, Paper, and Food. *ACS Nano* **2018**, *12* (3), 2176−2183.
(41) de Farias, D. M.; Pradela-Filho, L. A.; Arantes, I. V. S.; Gongoni, J. L. M.; Veloso, W. B.; Meloni, G. N.; Paixão, T. R. L. C. Sulfanilamide Electrochemical Sensor Using Phenolic Substrates and CO2 Laser Pyrolysis. *ACS Appl. Mater. Interfaces* **2023**, *15* (48), 56424−56432.
(42) Silva, E. M.; Takeuchi, R. M.; Santos, A. L. Carbon Nanotubes for Voltammetric Determination of Sulphite in Some Beverages. *Food Chem.* **2015**, *173*, 763−769.
(43) Li, Z.; Jiang, M.; Lu, D.; Wang, Y.; Li, H.; Sun, W.; Long, J.; Jeerapan, I.; Marty, J. L.; Zhu, Z. Nonenzymatic Glucose Electrochemical Sensor Based on Pd−Cu Bimetallic Aerogels. *Talanta* **2025**, *287*, 127641.
(44) Chiu, Y. H.; Rinawati, M.; Chang, L. Y.; Guo, Y. T.; Chen, K. J.; Chiu, H. C.; Lin, Z. H.; Huang, W. H.; Haw, S. C.; Yeh, M. H. Carbon Nitride Quantum Dots/Polyaniline Nanocomposites for Non-Invasive Glucose Monitoring Using Wearable Sweat Biosensor. *ACS Appl. Nano Mater.* **2025**, *8*, 2340.
(45) Zhang, Y.; Chen, J.; Wang, H.; Gao, X.; Niu, B.; Li, W.; Wang, H. Electrochemical Biosensor Based on Copper Sulfide/Reduced Graphene Oxide/Glucose Oxidase Construct for Glucose Detection. *Anal. Biochem.* **2025**, *696*, 115696.
(46) Liu, P. P.; Lau, S. F.; Ding, C. F. Non-Enzymatic Low-Level Glucose Detection Electrode Fabricated via Single-Step Laser-Induced Forward Transfer. *J. Mater. Chem. A* **2024**, *13*, 573−586.
(47) Uruc, S.; Gorduk, O.; Sahin, Y. Construction of Nonenzymatic Flexible Electrochemical Sensor for Glucose Using Bimetallic Copper Ferrite/Sulfur-Doped Graphene Oxide Water-Based Conductive Ink by Noninvasive Method. *ACS Appl. Bio Mater.* **2025**, *8*, 1451.
(48) Chen, Y.; Sun, Y.; Li, Y.; Wen, Z.; Peng, X.; He, Y.; Hou, Y.; Fan, J.; Zang, G.; Zhang, Y. A Wearable Non-Enzymatic Sensor for Continuous Monitoring of Glucose in Human Sweat. *Talanta* **2024**, *278*, 126499.
(49) Wu, P.; Fan, J.; Tai, Y.; He, X.; Zheng, D.; Yao, Y.; Sun, S.; Ying, B.; Luo, Y.; Hu, W.; Sun, X.; Li, Y. Ag@TiO2 Nanoribbon Array: A High-Performance Sensor for Electrochemical Non-Enzymatic Glucose Detection in Beverage Sample. *Food Chem.* **2024**, *447*, 139018.
(50) Ahamad, N.; Banerjee, S.; Wei, C. C.; Lu, K. C.; Khedulkar, A. P.; Jian, W. B.; Mahmood, S.; Chu, C. W.; Lin, H. C. Flexible Non-Enzymatic Glucose Sensors: One-Step Green Synthesis of NiO Nanoporous Films via an Electro-Exploding Wire Technique. *ACS Appl. Mater. Interfaces* **2024**, *16*, 64494.

https://doi.org/10.1021/acsaelm.5c00862
ACS Appl. Electron. Mater. XXXX, XXX, XXX−XXX

(51) Sheng, L.; Tan, H.; Zhu, L.; Liu, K.; Meng, A.; Li, Z. In Situ Anchored Ternary Hierarchical Hybrid Nickel@cobaltous Sulfide on Poly(3,4-Ethylenedioxythiophene)-Reduced Graphene Oxide for Highly Efficient Non-Enzymatic Glucose Sensing. *Microchim. Acta* **2024**, *191* (5), 267.

https://doi.org/10.1021/acsaelm.5c00862
ACS Appl. Electron. Mater. XXXX, XXX, XXX−XXX